maximum: a sink for atmospheric CO_2?

Wolfgang Ludwig [*], Philippe Amiotte-Suchet [1], Jean-Luc Probst

Ecole et Observatoire des Sciences de la Terre (EOST) ULP / CNRS, Centre de Géochimie de la Surface 1, rue Blessig, 67084 Strasbourg Cedex, France

Abstract

It has been proposed that increased rates of chemical weathering and the related drawdown of atmospheric CO_2 on the continents may have at least partly contributed to the low CO_2 concentrations during the last glacial maximum (LGM). Variations in continental erosion could thus be one of the driving forces for the glacial/interglacial climate cycles during Quaternary times. To test such an hypothesis, a global carbon erosion model has been applied to a LGM scenario in order to determine the amount of CO_2 consumed by chemical rock weathering during that time. In this model, both the part of atmospheric CO_2 coming from silicate weathering and the part coming from carbonate weathering are distinguished. The climatic conditions during LGM were reconstructed on the basis of the output files from a computer simulation with a general circulation model. Only the predicted changes in precipitation and temperature have been used, whereas the changes in continental runoff were determined with an empirical method. It is found that during the LGM, the overall atmospheric CO_2 consumption may have been greater than today (by about 20%), mainly because of greater carbonate outcrop area related to the lower sea level on the shelves. This does not, however, affect the atmospheric CO_2 consumption by silicate weathering, which alone has the potential to alter atmospheric CO_2 on the long-term. Silicate weathering and the concomitant atmospheric CO_2 consumption decreased together with a global decrease of continental runoff compared to present-day (both by about 10%). Nevertheless, some uncertainty remains because the individual lithologies of the continental shelves as well as their behavior with respect to chemical weathering are probably not well enough known. The values we present refer to the ice-free continental area only, but we tested also whether chemical weathering under the huge ice sheets could have been important for the global budget. Although glacial runoff was considerably increased during LGM, weathering under the ice sheets seems to be of minor importance.

Keywords: Atmospheric CO_2; Last glacial maximum; Chemical weathering

1. Introduction

Continental erosion represents a permanent transfer of carbon from the atmosphere to the oceans. Atmospheric/soil CO_2 is consumed both by organic matter formation and by chemical rock weathering, and subsequently discharged as dissolved organic

[*] Corresponding author. CEFREM, Université de Perpignan, 52 avenue de Villeneuve, 66860 Perpignan Cedex, France. Fax: +33-4-68-66-20-96; e-mail: ludwig@univ-perp.fr

[1] Present address: Laboratoire GéoSol, Centre des Sciences de La Terre Université de Bourgogne, 6, boulevard Gabriel, 21000 Dijon, France.

carbon, particulate organic carbon, and dissolved inorganic carbon to the oceans by rivers. The latter occurs mainly in the form of bicarbonate ions (HCO_3^-). In the long-term, the consumption of atmospheric CO_2 resulting from carbonate weathering on the continents is balanced in relatively short time scales by carbonate sedimentation in the oceans, where all CO_2 is released back to the ocean/atmosphere system. This is not the case for all CO_2 consumed by silicate weathering or by organic matter erosion. Here, a part of this carbon is lost to the lithosphere by carbonate precipitation and organic matter sedimentation, and only returns to the ocean/atmosphere system via metamorphism/volcanism and by the slow oxidation of old organic carbon in sedimentary rocks. Because the latter processes strongly depend on the tectonic activity on Earth, this lithospheric release of CO_2 can be quite variable over geological time scales.

Evidence from polar ice cores reveals a close coupling of the level of CO_2 in the atmosphere and global climate over at least the last 250,000 years (e.g., Neftel et al., 1988; Barnola et al., 1989; Alley et al., 1993), although it remains uncertain how sensitive climate is to variations in atmospheric CO_2, and to what extent these variations cause rather than result from climate change. Nevertheless, it has been widely accepted that changing the atmospheric CO_2 consumption by continental erosion can have an influence on climate on Earth, but some controversy about the involved mechanisms exists. On the one hand, it was proposed that continental erosion should act as a negative feedback to global temperature change (e.g., Walker et al., 1981; Berner et al., 1983), which is mainly controlled by the rate of sea floor spreading and hence an increase of volcanic outgassing of CO_2. Assuming that a higher global temperature causes more weathering, this process should bring atmospheric CO_2 again down to lower levels, and vice versa. Berner (1991, 1994) showed that such a mechanism could explain the general climatic variations observed during Phanerozoic times. On the other hand, Raymo et al. (1988) and Raymo (1994) suggested that the long-term removal rate of CO_2 from the atmosphere by chemical weathering is rather a function of relief than other factors, and that atmospheric temperature exerts only a weak control on global chemical erosion rates. They postulated that the global cooling during the late Cenozoic may be related to the built-up of the Tibetan plateau as a result of the collision of India and Asia, leading to a considerable increase of atmospheric CO_2 consumption by continental erosion.

The above mentioned processes operate on a multimillion-year time scale, but weathering may also have an influence on climate in much shorter time scales. In particular, continental erosion has been discussed as a potential candidate for being involved in the glacial/interglacial climate cycles during Quaternary times. Using an 11-box model for the oceanic carbon cycle, Munhoven and François (1996) showed that an increase of chemical silicate weathering by a factor of 2 to 3.5 during the last glacial maximum (LGM) could result in variations of atmospheric CO_2 that are close to those documented by ice cores. They justify such an assumption by the findings of Froelich et al. (1992), indicating considerably greater river fluxes of dissolved silica for the LGM than for the present-day. Gibbs and Kump (1994) confirmed the trend of generally increased weathering rates during the LGM, although they found this increase to be less important than that postulated by Munhoven and François (1996), and mainly to be related to an increase of carbonate erosion on the emerged shelves.

The purpose of this paper is to test the hypothesis of increased chemical weathering rates and river bicarbonate fluxes during the LGM. A global carbon erosion model that has been developed to simulate the present-day river fluxes (Amiotte-Suchet and Probst, 1995) was applied to a LGM scenario in order to determine the amount of atmospheric CO_2 consumed by the chemical weathering of rocks during that time. Contrary to the modelling study of Gibbs and Kump (1994), in our model both the CO_2 consumption by silicate weathering and by carbonate weathering is distinguished. It is therefore possible to test whether silicate weathering especially may have been sensitive to the changes in the environmental conditions during the LGM.

2. Data and methods

2.1. Model description

The fluxes of atmospheric CO_2 consumed by rock weathering (in the following F_{CO_2} for absolute val-

ues, and $F^s_{CO_2}$ for specific values, i.e., fluxes divided by the corresponding area) are mainly a function of runoff and of the rock type that is drained by the surface waters. This could been shown by Amiotte-Suchet and Probst (1993a,b, 1995), and by Amiotte-Suchet (1995) using data published by Meybeck (1986) about runoff and HCO_3^- concentrations in 232 monolithologic watersheds in France. The watersheds were grouped into six lithological classes representative for the major rock types outcropping on the continents, and the empirical relationships between $F^s_{CO_2}$ and runoff intensity (Q) were determined for each of the six classes. A linear relationship between $F^s_{CO_2}$ and Q for each rock type was found. Then, these relationships were validated on the level of large river basins. According to the stoichiometry of the weathering reactions, F_{CO_2} is considered to be equal to the HCO_3^- fluxes in waters draining silicate rocks, and to be equal to half of the HCO_3^- fluxes in waters draining carbonate rocks. These relationships can be seen, for example, in the following equations for the hydrolysis of albite (Eq. (1)) and for the dissolution of calcite (Eq. (2)):

$$2NaAlSi_3O_8 + 2CO_2 + 11H_2O \rightarrow Al_2Si_2O_5(OH)_4 + 2HCO_3^- + 2Na^+ + 4H_4SiO_4 \quad (1)$$

$$CaCO_3 + CO_2 + H_2O \rightarrow Ca^{2+} + 2HCO_3^- \quad (2)$$

For a given runoff intensity, $F^s_{CO_2}$ varies considerably for different rock types. $F^s_{CO_2}$ is 17 times greater for carbonate rocks, the rock type with the greatest specific CO_2 consumption, than for plutonic and metamorphic rocks, the rock type with the lowest specific CO_2 consumption. In the order of decreasing specific CO_2 consumption, the six rock types can be classified as follows: carbonate rocks, shales, basalts and gabbros, acid volcanic rocks, sands and sandstones, and plutonic and metamorphic rocks. Together, these relationships form the Global Erosion Model for atmospheric CO_2 consumption by rock weathering—GEM-CO_2 (Amiotte-Suchet and Probst, 1995). Bluth and Kump (1994) investigated CO_2 consumption by rock weathering based on data from different rivers and found similar relationships. Note that the present-day distribution of F_{CO_2} on the continents calculated by Amiotte-Suchet and Probst (1995) is available via ftp in a spatial resolution of $1° \times 1°$ longitude/latitude at the Carbon Dioxide Information Analysis Centre CDIAC (ftp cdiac.esd.ornl.gov/pub/db1012).

2.2. Reconstruction of the LGM climate

For the simulation of the Earth's climate prevailing during the LGM, we used in this study the monthly temperature and precipitation climatologies calculated by the ECHAM2 general circulation model (GCM). They exist both for a LGM simulation run (*lgm*) and for the corresponding present-day control run (*contr*), and they are available via ftp from the Deutsches Klima Rechenzentrum (Hamburg, Germany). More details on the ECHAM2 model are given by Lautenschlager and Herterich (1990), and by Lautenschlager (1991). Esser and Lautenschlager (1994) used the same model in order to estimate the change of carbon in the terrestrial biosphere from LGM to present with a global carbon cycle model. Since these ECHAM2 climatologies only exist in the $5.625° \times 5.625°$ longitude/latitude resolution of the model (so-called T21 resolution), the following algorithm was applied to derive $0.5° \times 0.5°$ grid point climatologies from the model files:

$$ValM_i = ValO_i \times ValM_j / (ValO_i)_j \quad (3)$$

ValM is either the monthly temperature (K) or precipitation (mm) value of the model; ValO is the corresponding value of the present-day temperature and precipitation data sets; and i and j are indices for the grid points in the $0.5° \times 0.5°$ (i) and in the T21 (j) resolution, respectively. As present-day data sets, we used the data of Legates and Willmott (1992) for temperature and for the monthly precipitation values (in percent of the annual values), whereas for mean annual precipitation a digitized and gridded version of the Atlas of World Water Balance of Korzoun et al. (1977) was used. $(ValO_i)j$ is the area-weighted average of all i that fall into j. Because this is a common practice also in other studies (e.g., Esser and Lautenschlager, 1994; Gibbs and

Kump, 1994), the final LGM climatologies were then obtained by subtracting the ECHAM2-derived anomalies from the present-day distributions according to:

$$\mathrm{ValO}_{(\mathrm{lgm})i} = \mathrm{ValO}_{(\mathrm{present-day})i} - \left(\mathrm{ValM}_{(\mathrm{contr})i} - \mathrm{ValM}_{(\mathrm{lgm})i}\right) \quad (4)$$

For precipitation, it could happen that Eq. (2) yields negative values. In these cases, the grid point values were set to 0. Esser and Lautenschlager (1994) derived the LGM precipitation data set in their study by applying the relative changes between the LGM and control run of the ECHAM2 model to the actual precipitation distribution, and not the absolute changes. This method avoids negative values, but it risks altering the global precipitation change predicted by the model with respect to the absolute values. None of the methods is without shortcomings. Note that the method we applied respects the absolute amount of precipitation change predicted by ECHAM2, except for the grid elements which are set to 0. Cutting off negative values overestimates to some extent the global LGM precipitation. In the LGM data set we created, this overestimation is about 1.5% of total precipitation, which is globally of small importance, confirming the applicability of our method.

When applied to the total continental area (about 152×10^6 km^2 for present-day and 173×10^6 km^2 for the LGM), the so-created LGM climatologies show a global cooling of 6.7°C compared to present-day (from 9.6 to 2.9°C), and a reduction of global precipitation of 77 mm (from 817 to 740 mm). Both the changes in continental area during the LGM related to the sea level fall as well as the appropriate LGM ice-coverage of the continents were taken from the reconstructions of Peltier (1994). These reconstructions exist as $1° \times 1°$ longitude/latitude global data files in 1000 year intervals since the LGM and are available via ftp from the World Centre for Paleoclimatology/National Geophysical Data Centre (Boulder, USA). We interpolated all data files to a $0.5° \times 0.5°$ longitude/latitude grid point resolution since we did all our calculations in this finer resolution. For the present-day situation, we followed the vegetation map of Olson et al. (1983) in order to define which of the Earth's $0.5° \times 0.5°$ grid points belong to the continents, and which belong to the oceans. Also the present-day extension of the polar ice sheets was taken from this data set. Finally, all fluxes we calculated refer to the exoreic parts of the continents only. Here we assumed that the endoreic regions during the LGM have been the same as today.

2.3. Determination of continental runoff

Among all potential controlling factors, mean annual runoff is globally the most important for the CO_2 consumption by rock weathering on the continents (Probst, 1992; Amiotte-Suchet and Probst, 1993a,b, 1995; Probst et al., 1994a; Amiotte-Suchet, 1995). The reliability of all simulations dealing with weathering rates and river carbon fluxes therefore strongly depends on the accuracy of the method applied to determine this parameter. From the ECHAM2 output files, runoff intensity can be derived by taking the difference between the precipitation and evaporation fields, but this value turns out to be negative many times, which makes this method less suitable for the determination of runoff during the LGM. For this reason, we derived this parameter by an empirical method based upon multiple regression analyses with the digitized and gridded runoff maps of Korzoun et al. (1977) and a great number of global environmental data sets (Ludwig and Probst, 1998).

In this modelling (Ludwig, in press), precipitation and temperature (which is uniquely used to derive potential evapotranspiration according to Holdridge, 1959), are the main parameters determining runoff. In agreement with the empirical relationship proposed by Pike (1964), it can be shown that the mean annual runoff ratio (RR, runoff divided by precipitation) generally increases the more precipitation exceeds potential evapotranspiration:

$$\mathrm{RR} = 1 - 1/\left(1 + (\mathrm{APPT}/\mathrm{APE})^2\right)^{0.5} \quad (5)$$

APPT is the mean annual precipitation total (mm), and APE the mean annual potential evapotranspiration (mm). In addition, large seasonal variability in precipitation can also increase the runoff ratio compared to a more uniform precipitation distribution. We characterized this parameter by using a slightly

modified form of the precipitation index originally proposed by Fournier (1960). Therefore, we named it Four (see Ludwig et al., 1996a). Finally, it is important to point out that morphology also represents a non-negligible controlling factor for runoff. Given the same temperature and precipitation values, greater slope increases runoff ratio, while greater elevation decreases it. The effect of basin slope is especially important in this respect, leading to considerably greater correlation coefficients than using the climatic variables alone. The fact that elevation has been retained in our empirical modelling may directly relate to the shortcoming of the method to estimate potential evapotranspiration from temperature data only (Ludwig, in press).

For all continental grid points, the following equation describes the relationship best:

$$RR = 0.73\,RR_{PIKE} + 1.06\,Slope + 0.78 \times 10^{-3}\,Four - 0.82 \times 10^{-4}\,Elev - 0.10 \quad (6)$$

RR_{PIKE} is the theoretical runoff ratio calculated according to Eq. (5), Slope is the mean grid point slope in radians (Moore and Mark, 1986), Four is in millimeters, and Elev is the modal grid point elevation in meters (Fleet Numerical Oceanography Center, 1992). We further grouped the grid points according to the major climate types to which they belong and repeated the regressions within these subgroups. In all cases, the above given parameters were found to be the dominant controlling factors in the same order as in Eq. (5), although the regression coefficients naturally varied to some extent. Only in the tundra and taiga climate was Four not found to be significant, which can be explained with the important contribution of snow melt to runoff in this climate type (seasonal variability of precipitation should be only of minor importance when a considerable amount of precipitation is temporarily stored as snow).

The advantage of this empirical modelling is that it allows a relative easy prediction of continental runoff with high precision. A validation with a set of 60 major world river basins (Ludwig and Probst, 1998) reveals for the present-day situation a correlation coefficient between the empirically determined

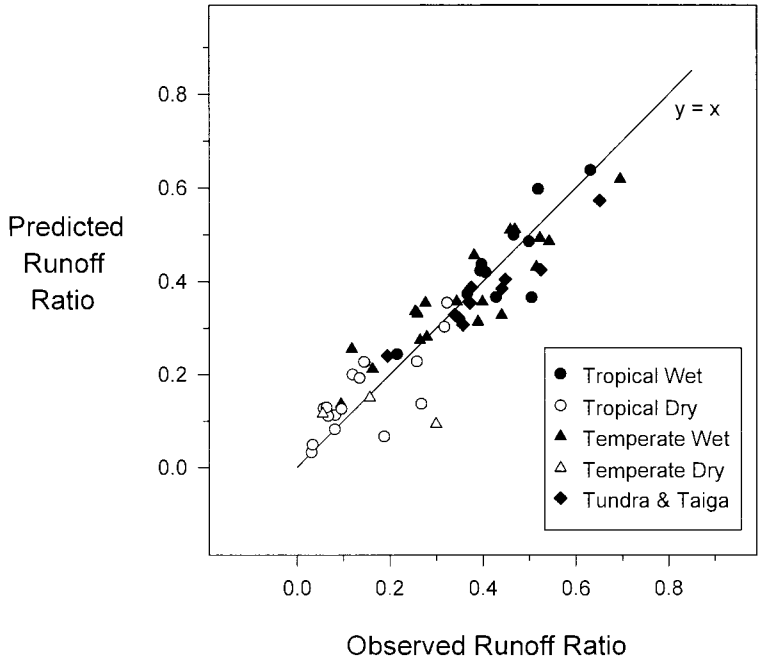

Fig. 1. Comparison of the mean runoff ratio empirically determined with the mean runoff ratio according to Korzoun et al. (1977) for 60 major river basins.

RR and the RR resulting from the runoff and precipitation maps of Korzoun et al. (1977) of $r^2 = 0.85$ (Fig. 1). The correlation coefficient for the resulting runoff intensities (according to $Q = \mathrm{RR} \times$ mean annual precipitation) is $r^2 = 0.97$.

3. Results and discussion

3.1. Atmospheric CO_2 consumption at the present-day

When GEM-CO_2 is applied to the total ice-free and exoreic continental area on the basis of a global lithological map created by Amiotte-Suchet (1995) and a global data set for drainage intensity (Korzoun et al., 1977), the model result yields a total amount of 0.23 gigatons of atmospheric carbon per year (Gt C year^{-1}) that is discharged to the present-day oceans. The corresponding water flux is 41750 km^3 year^{-1}. About 61% of F_{CO_2} is due to silicate weathering, and about 39% due to carbonate weathering, which means that an additional amount of 0.09 Gt C year^{-1} enters the oceans from the dissolution of carbonate minerals. These values compare well with other literature estimates, confirming the applicability of GEM-CO_2. More details on the spatial distribution of $F^s_{CO_2}$ can be found in Probst et al., 1994b; Probst et al., in press; Amiotte-Suchet and Probst, 1995; Ludwig et al., 1996b, 1998.

3.2. Atmospheric CO_2 consumption during the LGM

In order to calculate the corresponding fluxes for the LGM, we assumed that the lithological and morphological characteristics of the continents during the LGM were the same as for today. We therefore only changed in our simulation the data set for runoff intensity derived from the reconstructed LGM climatologies (see above). The major problem is that the morphological and lithological characteristics for the grid elements which became land area during the LGM as a result of the lower sea level (in the following: 'new' continental grid points—see Table 1) are not known. Consequently, neither our empirical modelling of runoff nor GEM-CO_2 can be applied to these grid elements, and it is thus not possible to calculate one definitive value for global F_{CO_2} during the LGM. Thus, as an approximation, we used the following method to estimate the global CO_2 consumption by chemical rock weathering. For each climate type, for each continent, and for each of the continental areas which drain to the different ocean basins, the average F_{CO_2} and runoff values were calculated only on the basis of the grid points that belong to the exoreic and ice-free continental area both for the present-day and for the LGM (in the following: 'old' continental grid points—see Table 1). At the same time, runoff on the new grid points was estimated by a triangular interpolation of the runoff ratios between the old continental grid points over the oceans and the applying of them to the LGM precipitation values (also other methods such as the application of Eq. (5) have been tested, but this results only in minor differences). The total F_{CO_2} fluxes within each category can then be established according to:

$$F_{CO_2} = \left(F^s_{CO_2-\mathrm{old}} \times \mathrm{Area}_{\mathrm{old}}\right) + \left(F^s_{CO_2-\mathrm{old}} \times \mathrm{Area}_{\mathrm{new}} \times Q_{\mathrm{new}}/Q_{\mathrm{old}}\right) \quad (7)$$

The units are Tg C year^{-1} for F_{CO_2}, t km^{-2} year^{-1} for $F^s_{CO_2}$, $10^6 \times \mathrm{km}^2$ for Area, and mm for Q. Finally, the arithmetic mean of the global F_{CO_2} values in the three categories was selected as the best estimate for the global atmospheric CO_2 consumption by chemical rock weathering during LGM (Table 2).

The above described method assumes that $F^s_{CO_2}$ on the new grid points linearly increased or decreased according to the variations in runoff intensity compared to the old continental grid points. This procedure can be justified by the dominant role of continental runoff as a controlling factor for F_{CO_2} (see above), but it is only true if the average lithology of the new continental grid points is about the same as on the old grid points. The latter is naturally questionable. For this reason, we also made several sensitivity runs by assuming different types of lithology on the new continental grid points in order to get an idea about the resulting differences in the amount of atmospheric CO_2 consumption by chemical rock weathering during the LGM (Table 3). Differences between the sensitivity runs and the above described

Table 1
Comparison of the distribution of present-day continental area and major climate types with the situation during the last glacial maximum

	Present-day area[a]		Last glacial maximum area[a]			
	Total (10^6 km^2)	Exoreic, no ice (10^6 km^2)	Total (10^6 km^2)	Exoreic, no ice		
				Total (10^6 km^2)	'Old' (10^6 km^2)[b]	'New' (10^6 km^2)[c]
Polar (ice covered)	15.26	–	42.55	–	–	–
Polar (no ice)	3.89	3.89	6.33	6.10	3.71	2.39
Tundra and Taiga	24.09	23.21	20.74	17.99	17.12	0.87
Temperate Dry	16.18	9.63	15.88	10.04	9.28	0.76
Temperate Wet	18.56	16.92	12.32	11.15	9.69	1.46
Tropical Dry	25.53	21.79	23.61	20.77	17.85	2.92
Tropical Wet	25.07	24.93	26.08	25.99	22.99	3.00
Desert	23.88	5.96	25.35	7.51	6.61	0.90
Total	152.47	106.33	172.86	99.55	87.24	12.31
Africa	33.00	18.29	33.88	19.17	18.30	0.87
Europe	12.70	9.56	16.19	7.16	6.16	1.00
North America	25.40	23.02	29.61	12.07	10.27	1.80
South America	18.16	17.73	19.62	18.65	17.29	1.36
Asia	41.03	32.52	48.34	36.73	30.77	5.96
Australia	8.33	4.48	9.66	5.77	4.45	1.32
Antarctics	13.85	0.73	15.56	–	–	–
Total	152.47	106.33	172.86	99.55	87.24	12.31
Arctic Ocean	17.55	16.98	22.42	11.90	10.75	1.15
North Atlantic	38.86	27.30	43.31	19.37	17.18	2.19
South Atlantic	18.55	16.96	19.58	17.86	16.85	1.01
Pacific	29.98	21.02	35.24	24.00	19.12	4.88
Indian Ocean	23.90	16.59	26.63	19.33	16.62	2.71
Mediterranean	9.77	6.74	10.13	7.09	6.73	0.36
Below 60° South	13.85	0.73	15.56	–	–	–
Total	152.47	106.33	172.86	99.55	87.24	12.31

[a] For the ocean basins, this is the continental area that is drained to the different basins.
[b] This is the area that is continental both for present-day and for LGM.
[c] This is the area that is continental only for LGM due to the lower sea level.

method, therefore, can help to estimate the importance of shelf lithology on global F_{CO_2}.

The most plausible way to increase river carbon fluxes at the global scale would be to increase continental area concomitantly with an increase of runoff. Assuming that weathering is negligible under ice sheets (this point is also discussed below), the effective erodible area of the continents was not much different during the LGM than today because the loss of area caused by the extension of the ice sheets was more or less compensated for by a greater exposure of shelf area due to the sea level fall (Fairbanks, 1989). In our LGM scenario this area decreases slightly by about 6% (Table 1). A crucial question for the atmospheric CO_2 consumption by chemical rock weathering during LGM is hence whether the amount of runoff on the continents has been significantly different.

Due to a steeper temperature gradient towards the poles, the humid climate zones of the mid and high latitudes were considerably smaller during the LGM compared to today (Fig. 2). Note from Table 1 that the temperate wet and the tundra and taiga climates were reduced by about 34% and 22%, respectively. This is not without consequences for the total amount of water running off the continents, since both climate types are important contributors to global runoff (Table 2). Consequently, runoff on the old continen-

Table 2
Continental runoff and atmospheric CO_2 consumption by rock weathering during the last glacial maximum

	Runoff (km^3)			F_{CO_2} (Tg C $year^{-1}$)			F_{CO_2} from silicate weathering	
	Old area[a]	New area[b]	Total	Old area[a]	New area[b]	Total	(Tg C $year^{-1}$)	% of today
Polar (no ice)	1108	1105	2213	9.11	9.09	18.19	9.80	489.9
Tundra and Taiga	3782	701	4483	21.68	4.02	25.70	16.52	67.8
Temperate Dry	927	69	996	7.38	0.55	7.93	2.36	102.6
Temperate Wet	5118	874	5992	31.25	5.34	36.58	17.47	75.7
Tropical Dry	2363	773	3135	15.11	4.94	20.05	7.96	83.7
Tropical Wet	17624	3551	21174	89.85	18.10	107.95	82.60	105.1
Desert	203	25	228	1.32	0.17	1.48	0.64	318.9
Total	31124	7097	38221	175.69	42.19	217.89	137.35	98.1
Africa	3784	226	4010	14.01	0.84	14.85	6.64	100.6
Europe	1641	570	2211	13.75	4.77	18.52	8.76	78.3
North America	3528	1140	4668	22.24	7.19	29.42	18.18	78.1
South America	9541	687	10228	47.70	3.44	51.14	43.50	97.1
Asia	12046	4138	16184	76.29	26.21	102.50	57.08	110.7
Australia	584	336	920	1.71	0.98	2.69	2.67	127.1
Antarctics	–	–	–	–	–	–	–	–
Total	31124	7097	38221	175.69	43.42	219.11	136.84	98.0
Arctic Ocean	1362	106	1469	7.19	0.56	7.76	5.86	41.1
North Atlantic	9794	1534	11328	56.89	8.91	65.80	48.26	97.9
South Atlantic	4400	295	4695	16.06	1.08	17.14	11.11	103.8
Pacific	9141	4155	13296	56.56	25.71	82.27	52.80	110.7
Indian Ocean	5491	966	6457	30.57	5.37	35.94	15.68	118.0
Mediterranean	935	42	977	8.42	0.37	8.79	4.24	88.4
Below 60° South	–	–	–	–	–	–	–	–
Total	31124	7097	38221	175.69	42.01	217.70	137.96	98.4
Best estimate				175.69	42.54	218.23	137.38	98.2

The values are based on the assumption that average lithology on the new grid points is the same as that on the old grid points.
[a]Area that is continental both for present-day and for LGM.
[b]Area that is continental only for LGM due to the lower sea level (emerging shelves).

tal grid points was globally reduced by about 9%. This general picture of on average more arid conditions during the LGM is also in agreement with observations. Reconstruction of vegetation distribution based on palynological, pedological, and sedimentological evidence globally indicates a greater

Table 3
Atmospheric CO_2 consumption by rock weathering during the last glacial maximum on the new grid points for different lithologies

Lithological character of the new continental grid points (emerging shelves)	Total F_{CO_2}				F_{CO_2} from silicate weathering	
	Old area (Tg C $year^{-1}$)[a]	New area (Tg C $year^{-1}$)	Total (Tg C $year^{-1}$)	% of today	(Tg C $year^{-1}$)	% of today
All sandstones	175.69	15.40	191.09	83.1	125.10	89.4
All carbonates	175.69	128.90	304.59	132.4	112.60	80.5
All shales	175.69	56.30	231.99	100.9	166.10	118.7
30°S–30°N carbonates, rest shales	175.69	105.80	281.49	122.4	132.20	94.5
30°S–30°N carbonates, rest sandstones	175.69	89.30	264.99	115.2	115.70	82.7

[a]See Table 2.

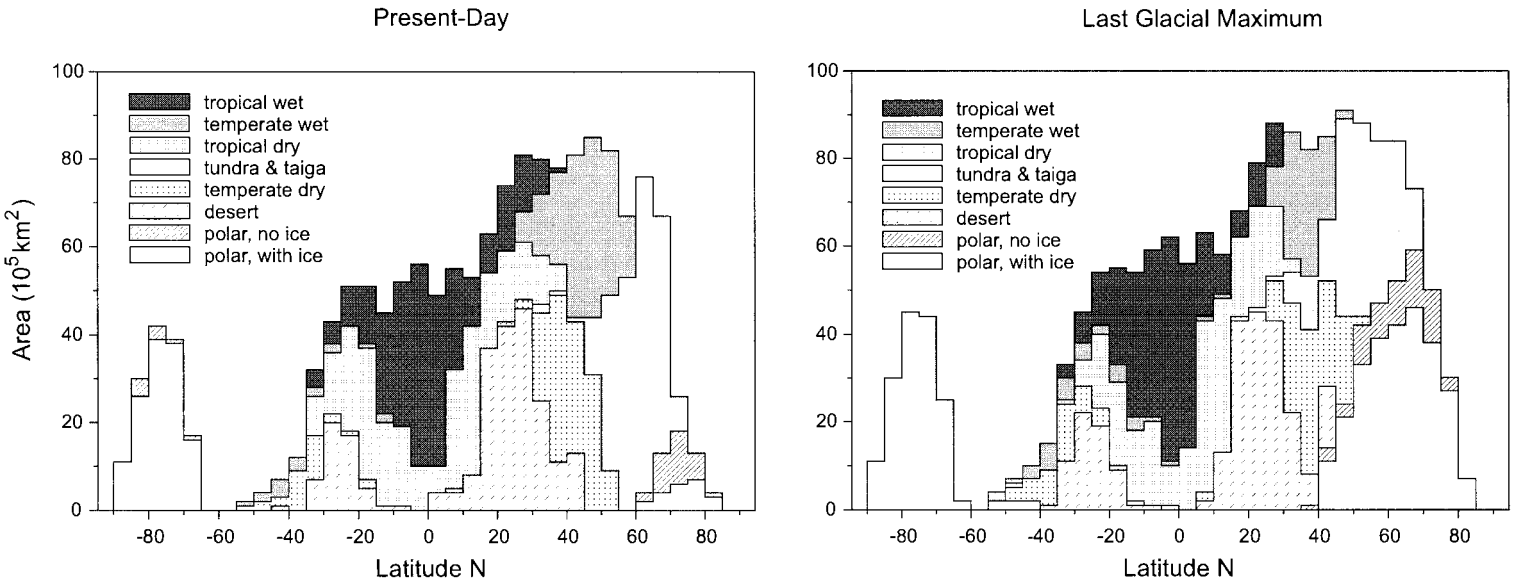

Fig. 2. Holospheric distribution of the major climate types on Earth at present, and as reconstructed for the last glacial maximum. Definition of the climate types is based only on temperature and precipitation data (Ludwig et al., 1996a).

aridity during the LGM than today (Adams et al., 1990; Adams and Faure, 1996). Also from palaeohydrological evidences, Starkel (1988) concluded that water discharge by rivers was generally lower during the LGM than today.

On the emerging shelves, however, runoff intensity was clearly greater than on the rest of the continents (by about 62%). This is mainly due to the fact that large parts of this area emerged in the tropics of the low latitudes, where by far most of the water runs off the continents (Table 2). Also in the high latitudes, runoff was locally increased, especially close to the margins of the ice sheets (such as the North Sea), where the GCM simulation results in a significant increase of precipitation compared to present-day. The high runoff intensity on the new continental grid points thus partly compensated for the greater aridity on the old grid points, but this effect on the whole is not strong enough to increase runoff. Thus, the total amount of water running off the continents was about 9% lower during the LGM than at present-day, and the more humid shelves hence only compensated for the reduction in the erodible continental area.

Consequently, application of GEM-CO_2 to the simulated LGM conditions results also in a reduction of the amount of atmospheric CO_2 consumed by rock weathering, at least as far as the old grid points are concerned. $F^{s}_{CO_2}$ was especially reduced in the tropical parts of South and Middle America, Africa, and SE Asia, as well as in many parts of North Asia (Fig. 3). However, the values were increased both in North America and northern Europe close to the ice-sheets, and in large parts of the southern hemisphere. Under the assumption that the average lithology on the new grid points was about the same as that on the old grid points, we calculate the global reduction of F_{CO_2} to be about 5% lower than the present-day value (Table 2). Although there is no fundamental difference in the share of F_{CO_2} coming from silicate weathering between today and the LGM, a slight increase of the relative importance of silicate weathering during the LGM can be noted (from 60.8% to 63.3%), and the global value for F_{CO_2} from silicate weathering remains about the same as that for today (-1%).

Assuming different rock types to be on the emerging shelves than on the rest of the continental area (Table 3) allows the total F_{CO_2} to vary substantially, that is between about -20% and $+30\%$ compared to the present-day value. Lowest values are found by allowing only sandstones to outcrop on the shelves, the rock type with the weakest specific CO_2 consumption. Greatest values result from an overall coverage of the exposed shelf by carbonates, the rock type with by far the greatest specific CO_2 consumption. In the latter case, however, F_{CO_2} from silicate weathering would only be about 80% of today's value.

It is interesting to compare our results with the results of Gibbs and Kump (1994) who investigated the changes of bicarbonate fluxes on glacial/interglacial time scales in a similar study as ours. Both studies are in a way complementary, since Gibbs and Kump proposed a global lithological map that is also valid for the emerging shelf grid points. However, they do not distinguish between the share of bicarbonates resulting from silicate weathering and that resulting from carbonate weathering. They found that river HCO_3^- fluxes during the LGM may have been with about 20% greater than today because of a greater exposure of carbonate rocks on the shelves, and that the global runoff value from the ice-free regions of the continents remained nearly unchanged.

Using the lithological map published by Gibbs and Kump (1994), we estimate the proportion of carbonates, shales, and sandstones on the emerging shelves to be about 45%, 40%, and 15% respectively. By far most of the carbonates are situated in the lower latitudes of 30°S to 30°N. When combining these estimates with our results (Table 3), GEM-CO_2 also predicts an increase of total F_{CO_2} of about 20% during the LGM, which is in good agreement with the study of Gibbs and Kump. At the same time, however, F_{CO_2} from silicate weathering alone is about 10% lower than that for the present-day. The latter percent is about equivalent to the reduction in continental runoff. This implies that F_{CO_2} from silicate weathering is probably more closely coupled to climate change (runoff) than F_{CO_2} from carbonate weathering, and is in disagreement with the idea of F_{CO_2} as one of the principal driving forces for lower atmospheric CO_2 during glacial times.

The above values given for an increase in total F_{CO_2} by about 20% together with a 10% decrease in F_{CO_2} from silicate weathering during the LGM may

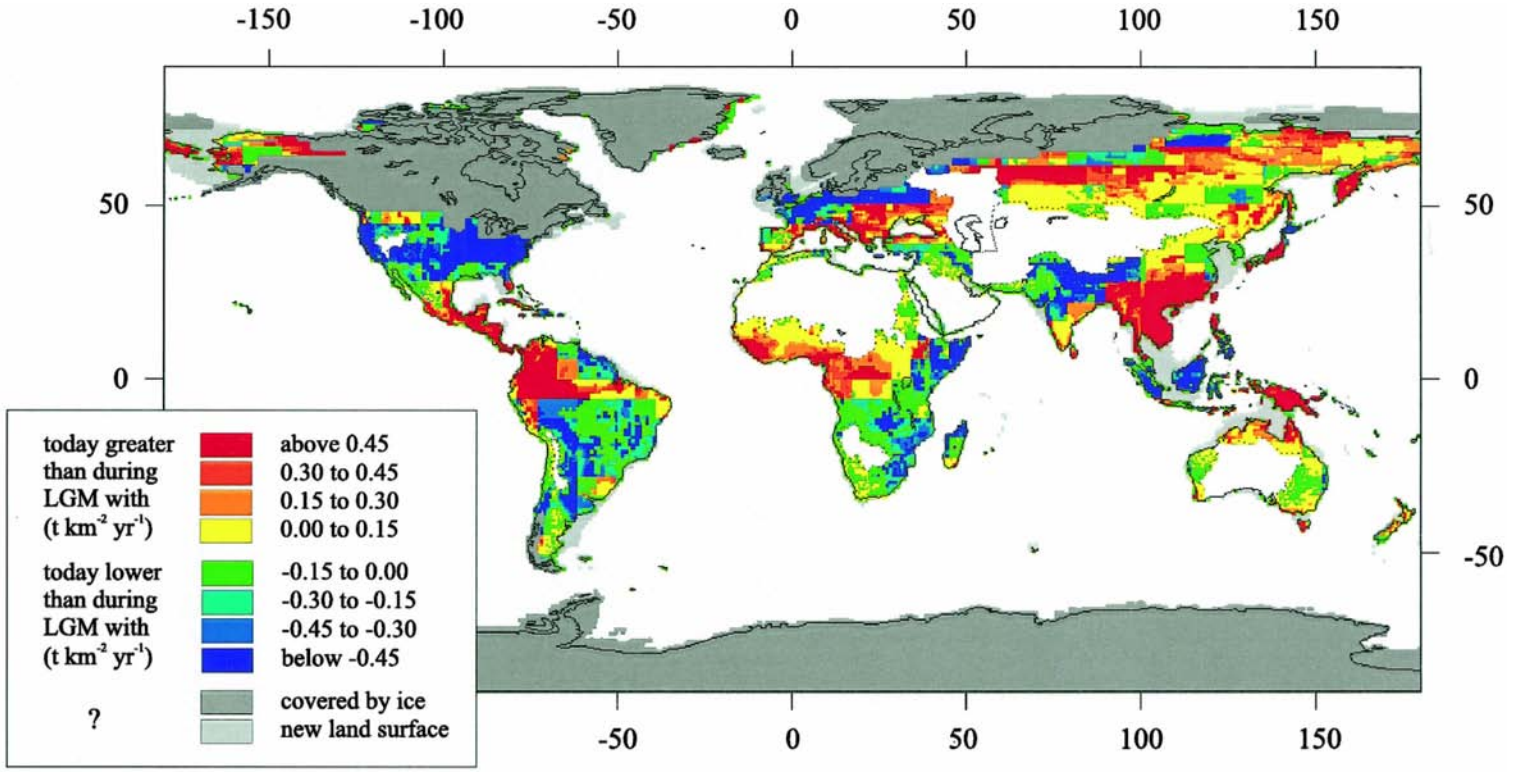

Fig. 3. Atmospheric CO_2 consumption by rock weathering: differences between present-day and the last glacial maximum. The white parts of the continents are endoreic.

be considered as best estimates on the basis of the data available for this study. Nevertheless, our results also show that the different types of lithology outcropping on the shelves can have a non-negligible effect on the global figures, and a refinement of our estimates requires more information on precise shelf lithology. Another major unknown is the exact nature of the weathering status of the sediments that are currently on the seafloor and which were exposed during the LGM. Having already been through the weathering cycle, it is not obvious that shelf sediments would undergo significant weathering if exposed (Gibbs and Kump, 1994).

3.3. Chemical weathering under the ice sheets

Another open question in our reconstruction of atmospheric CO_2 consumption during the LGM is whether the above assumption that no chemical weathering takes place underneath ice sheets is correct or not. Chemical weathering could have occurred at least at the ice sheet margins, where melt waters were in contact both with atmospheric CO_2 and large amounts of fine-grained glacial debris (Gibbs and Kump, 1994). When analysing melt waters from a Swiss glacier, Sharp et al. (1995) found chemical weathering rates substantially higher than the global average. They concluded that deglacial meltwater discharge pulses could remove considerable amounts of CO_2 from the atmosphere, and that glacially driven chemical weathering may have an important role in carbon cycling over glacial-interglacial time scales. If high consumption rates hold also for extended parts of the LGM ice sheets, the continental area subjected to chemical weathering was considerably greater for the LGM than for today, which is probably not a negligible term in our budgets.

In order to test such an hypothesis, we determined the amount of annual precipitation falling on the ice sheets during LGM on the basis of our precipitation data set. Compared to present-day, the specific value exactly doubled from 206 to 412 mm. Given the assumption that the extension and thickness of the ice sheets did not change from one year to another, this can be taken as a maximum value for the amount of glacial runoff within one year, except that it has to be reduced for the water lost by evaporation. From the present-day data of Korzoun et al. (1977), we estimate that the runoff ratio in glacial regions may be close to 0.9, although even this value is naturally somewhat speculative because of the scarcity of measurements in these regions. The runoff ratio during the LGM should have been lower because much of the northern ice was at lower latitudes, and evaporation should have been more important. Nonetheless, given the huge continental area that has been covered by the ice sheets (Table 1) and taking a runoff ratio of 0.9 means that glacial runoff could have been as great as 15750 km^3 $year^{-1}$ during the LGM. This value is about 3/4 of the runoff from the tropical wet climate (Table 2), and about six times the present-day value (2620 km^3 $year^{-1}$).

We then multiplied this value for glacial runoff times the average concentration of carbon coming from atmospheric CO_2 that was found in the study of Sharp et al. (1995). This value is an average of the two years of observation, about 1.12 mg C l^{-1}. The authors reported a nearly linear relationship between F_{CO_2} and Q in their data, so that this concentration should have been relatively constant in the waters they analyzed. Thus, the total amount of F_{CO_2} related to glacial weathering during the LGM is calculated as 17.6 Tg C $year^{-1}$, a value that is about 8% of F_{CO_2} on the rest of the continents in Table 2 (average lithology scenario). This value is an absolute maximum because it assumes that all of the glacial runoff water has been in contact with the underlying rocks. In reality, this is only the case for a small part of the water. At many places the ice sheets bordered directly on the sea (Fig. 3), and a considerable amount of glacial runoff may have occurred in the form of ice-calving. Moreover, extrapolating chemical weathering rates from valley glaciers to ice sheets is also highly questionable because the amount of meltwater production, the exposure of that water to atmospheric CO_2, and the amount of fresh reactive mineral surfaces created by abrasion under ice sheets would tend to differ substantially from that under small temperate glaciers (Hallet et al., 1996). Because of the much lower temperatures, the base of the ice sheets during the LGM were probably entirely frozen to its bed over large areas.

For these reasons, we conclude that the total amount of F_{CO_2} related to glacial weathering during the LGM probably was only a small part of the value

calculated above, and hence nearly negligible in our budgets. Of course, studies of solute yields from glaciated basins are relatively limited in numbers (Hallet et al., 1996), and more data are needed to improve our knowledge on glacial weathering rates. In this context it is also clear that comparing specific yields from glaciated basins with other regions or with global averages as done by Sharp et al. (1995) is not necessarily very meaningful because it does not take into account the large variability of runoff intensity and lithology that can exist. Note that the catchment investigated by Sharp et al. (1995) has a runoff intensity of about 2000 mm $year^{-1}$, which is nearly twice the value of the Amazon Basin, and five times the world average (Ludwig and Probst, 1998). It is questionable that such a value can be extrapolated to the large ice sheets during glacial stages. Consequently, when investigating chemical weathering in glacial environments, Anderson et al. (1997) reported that although catchments occupied by alpine glaciers yield cation denudation rates greater than the world mean rate, they do not exceed rates in catchments with similar water discharge. Silicate mineral denudation rates were found to be distinctly lower in glacier-covered catchments than in their non-glacial counterparts, leading the authors to conclude that the concomitant consumption of atmospheric CO_2 does not appear to be unusually rapid in glacier covered basins.

4. Conclusions

In this study, a global erosion model (GEM-CO_2) has been applied to LGM climate conditions reconstructed by a GCM simulation in order to predict the amount of atmospheric CO_2 consumed by rock weathering. It is found that total F_{CO_2} during the LGM was probably even greater than today, assuming that lithology on the emerging shelves was dominated by widely outcropping carbonates, together with shales, and, to a minor extent, sandstones. However, carbonate outcrops do not affect F_{CO_2} coming from silicate weathering, which alone has the potential to alter atmospheric CO_2 in the long-term. Silicate weathering and the concomitant atmospheric CO_2 consumption would decrease under this scenario. Assuming that the average lithology on the emerging shelves was the same as that on the rest of the continents would result in an overall atmospheric CO_2 consumption by silicate weathering that is about the same as that for the present-day. The values we calculated refer to the ice-free and exoreic continental area only, but we tested also the hypothesis of increased weathering fluxes under the huge ice sheets during the LGM. The latter seems to have a very small impact on the global CO_2 budget. Therefore, our results do not confirm the assumption of weathering to be one of the reasons for global cooling during glacial times, as this has been previously discussed in the literature, and are rather in agreement with the general idea of a negative coupling of weathering rates and global temperature on Earth (see Section 1).

The reliability of our findings is naturally strongly dependent on the reliability of the GCM outputs. Such computer simulations are still in an early stage of development, and there has been some discussion in the literature whether the prescribed sea surface temperatures normally used to constrain the simulations are too warm (Crowley, 1994; Broecker, 1995). This has to be kept in mind when looking at our results. Nevertheless, the prediction that the LGM world was more arid than today is confirmed by palynological, pedological, and sedimentological evidences. Finally, one has to point out that atmospheric CO_2 consumption by continental erosion does not only consist of the chemical weathering of rocks. The erosion of organic matter also represents a drawdown of CO_2 from the atmosphere. Quantitatively, this is even more important than the CO_2 consumption by rock weathering in the present-day carbon cycle (Ludwig et al., 1996b, 1998). Also variations in this flux have the potential to alter atmospheric CO_2 over longer time scales, especially when changes in the ratio of organic matter input to organic matter burial in sediments in the oceans are considered. Further studies on the role of continental erosion in the glacial/interglacial carbon cycle should therefore also include the behavior and fate of the river fluxes of organic matter.

Acknowledgements

This work was supported by funding from the Commission of the European Communities within

the project ‘European Study of Carbon in the Ocean, in the Biosphere, and in the Atmosphere’ (ESCOBA/Biosphere; contract no. ENV4-CT95-0111). This paperis a contribution to the ‘Working group weathering as a carbon sink’ of the INQUA commission ‘The Global Carbon Cycle’ and to the IGCP Project no. 404 ‘Terrestrial Carbon in the Past 125 kyear’.

References

Adams, J.M. and Faure, H., 1996. Changes in moisture balance between glacial and interglacial conditions: influence on carbon cycle processes. in: J. Branson, A.G. Brown, K.J. Gregory (Eds.), Global Continental Changes: the Context of Palaeohydrology. Geol. Soc. Spec. Publ. 115, pp. 27–42.

Adams, J.M., Faure, H., Laure-Denard, L., McGlade, J.M., Woodward, F.I., 1990. Increases in terrestrial carbon storage from the last glacial maximum to the present. Nature 348, 711–714.

Alley, R.B., Meese, R.B., Shuman, A.J., 1993. A new Greenland ice-core record from GISP2. Nature 366, 443–445.

Amiotte-Suchet, P., 1995. Cycle du carbone, érosion chimique des continents et transferts vers les océans. Sci. Géol. Mém., Strasbourg 97, 156.

Amiotte-Suchet, P., Probst, J.L., 1993a. Modeling of atmospheric CO_2 consumption by chemical weathering of rocks: Application to the Garonne Congo and Amazon basins. Chem. Geol. 107, 205–210.

Amiotte-Suchet, P., Probst, J.L., 1993b. Flux de CO_2 consommé par altération chimique continentale: influence du drainage et de la lithologie. C.R. Acad. Sci. Paris 317, 615–622.

Amiotte-Suchet, P., Probst, J.L., 1995. A global model for present day atmospheric/soil CO_2 consumption by chemical erosion of continental rocks (GEM-CO_2). Tellus 47 B, 273–280.

Anderson, S.P., Drever, J.I., Humphrey, N.F., 1997. Chemical weathering in glacial environments. Geology 25, 399–402.

Barnola, J.M., Raynaud, D., Korotkevitch, Y.S., Lorius, C., 1989. Vostok ice core provides 160000-year record of atmospheric CO_2. Nature 329, 408–414.

Berner, R.A., 1991. A model for atmospheric CO_2 over Phanerozoic time. Am. J. Sci. 291, 339–376.

Berner, R.A., 1994. GEOCARB II: a revised model of atmospheric CO_2 over Phanerozoic time. Am. J. Sci 294, 56–91.

Berner, R.A., Lasaga, A.C., Garrels, R.M., 1983. The carbonate-silicate geochemical cycle and its effect on atmospheric carbon dioxide over the past 100 millions years. Am. J. Sci. 283, 641–683.

Bluth, G.J.S., Kump, L.R., 1994. Lithologic and climatologic controls of river chemistry. Geochim. Cosmochim. Acta 58, 2341–2359.

Broecker, W.S., 1995. Cooling the tropics. Nature 376, 212–213.

Crowley, T.J., 1994. Pleistocene temperature changes. Nature 371, 664.

Esser, G., Lautenschlager, M., 1994. Estimating the change of carbon in the terrestrial biosphere from 18000 b.p. to present using a carbon cycle model. Environ. Pollut. 83, 45–53.

Fairbanks, R.G., 1989. A 17000 year glacio-eustatic sea level record: influence of glacial melting rates on the Younger Dryas event and deep-ocean circulation. Nature 342, 637–642.

Fleet Numerical Oceanography Center, 1992. Global elevation, terrain, and surface characteristics. Digital raster on a 10-min geographic (lat/long) 1080×2160 grid. in: NOAA/National Geopysical Data Center (Ed.), Global Ecosystems Database, Version 1.0 Disc (CD-ROM). National Geopysical Data Center, Boulder, CO.

Froelich, P.N., Blanc, V., Mortlock, R.A., Chillrud, S.N., 1992. River fluxes of dissolved silica to the oceans were higher during glacials: Ge/Si in diatoms, rivers, and oceans. Palaeoceanography 7, 739–767.

Gibbs, M.T., Kump, L.R., 1994. Global chemical erosion during the last glacial maximum and the present: sensivity to changes in lithology and hydrology. Palaeoceanography 9, 529–543.

Hallet, B., Hunter, L., Bogen, J., 1996. Rates of erosion and sediment evacuation by glaciers: a review of field data and their implications. Global and Planetary Change 12, 213–235.

Holdridge, L.R., 1959. Simple method for determining potential evapotranspiration from temperate data. Science 130, 572.

Korzoun, V.I., Sokolov, A.A., Budyko, M.I., Voskresensky, G.P., Kalinin, A.A., Konoplyantsev, E.S., Korotkevich, E.S., Lvovich, M.I., 1977. Atlas of World Water Balance. UNESCO Press, Paris, 36 pp.

Lautenschlager, M., 1991. Simulations of ice-age atmosphere—January and July means. Geol. Rdsch. 80, 513–534.

Lautenschlager, M., Herterich, K., 1990. Atmospheric response to ice age conditions: climatology near the Earth’s surface. J. Geophys. Res. 95, 22547–22557.

Legates, D.R., Willmott, C.J., 1992. Monthly average surface air temperature and precipitation: Digital raster on a 30 min geographic (lat/long) 360×720 grid. in: NOAA/National Geopysical Data Center (Ed.), Global Ecosystems Database, Version 1.0 Disc (CD-ROM). National Geopysical Data Center, Boulder, CO.

Ludwig, W. Continental erosion and river transport of organic carbon to the world’s oceans. Sci. Géol. Mém., Strasbourg, in press.

Ludwig, W., Probst, J.L., 1998. River sediment Discharge to the Oceans: present-day controls and global budgets. Am. J. Sci. 298, 265–295.

Ludwig, W., Amiotte-Suchet, P., Munhoven, G., Probst, J.L., 1998. Atmospheric CO_2 consumption by continental erosion: Present-day controls and implications for the last glacial maximum. Global and Planetary Change 16–17, 95–108.

Ludwig, W., Probst, J.L., Kempe, S., 1996a. Predicting the oceanic input of organic carbon by continental erosion. Global Biogeochem. Cycles 10, 23–41.

Ludwig, W., Amiotte-Suchet, P., Probst, J.L., 1996b. River discharges of carbon to the world’s oceans: determining local inputs of alkalinity and of dissolved and particulate organic carbon. C.R. Acad. Sci. Paris 323, 1007–1014.

Meybeck, M., 1986. Composition chimique des ruisseaux non pollués de France. Sci. Géol. Bull. 39, 3–77.

Moore, J.G., Mark, R.K., 1986. World slope map. EOS Trans. AGU 67, 1353–1356.

Munhoven, G., François, L.M., 1996. Glacial-interglacial variability of atmospheric CO_2 due to changing continental silicate rock weathering. J. Geophys. Res. 101 (D 16), 21423–21437.

Neftel, A., Oeschger, H., Staffelbach, T., Stauffer, B., 1988. CO_2 record in the Bird ice core, 50,000–5000 years b.p. Nature 331, 609–611.

Olson, J.S., Watts, J.A., Allison, L.J., 1983. Carbon in live vegetation of major world ecosystems. Report ORNL-5862, Oak Ridge Laboratory, Oak Ridge, TN, 164 pp.

Probst, 1992. Géochimie et hydrologie de l'érosion continentale. Mécanismes, bilan global actuel et fluctuations au cours des 500 derniers millions d'années. Sci. Géol. Mém., Strasbourg, 94, 161 pp.

Probst, J.L., Mortatti, J., Tardy, Y., 1994a. Carbon river fluxes and weathering CO_2 consumption in the Congo and Amazon river basins. Appl. Geochem. 9, 1–13.

Probst, J.L., Amiotte-Suchet, P., Ludwig, W., 1994b. Continental erosion and river transports of carbon to oceans. Trends Hydrol. 1, 453–468.

Probst J.-L., Ludwig W., Amiotte-Suchet P. Global modelling of CO_2 uptake by continental erosion and of carbon river transports to the oceans. Sci. Géol. Bull., 50, 1–4, Strasbourg, in press.

Peltier, W.R., 1994. Ice age palaeotopography. Science 265, 195–201.

Pike, J.G., 1964. The estimation of annual runoff from meteorological data in a tropical climate. J. Hydrol. 2, 116–123.

Raymo, M.E., 1994. The Himalayas, organic carbon burial, and climate in the Miocene. Paleoceanography 9, 399–404.

Raymo, M.E., Ruddiman, W.F., Froelich, P.N., 1988. Influence of late Cenozoic mountain building on ocean geochemical cycles. Geology 16, 649–653.

Sharp, M., Tranter, M., Brown, G.H., Skidmore, M., 1995. Rates of chemical denudation and CO_2 drawdown in a glacier-covered alpine catchment. Geology 23, 61–64.

Starkel, L., 1988. Global paleohydrology. Bull. Pol. Acad. Sci 36, 71–89.

Walker, J.C.G., Hays, P.B., Kasting, J.F.A., 1981. A negative feedback mechanism for the long term stabilisation of Earth's surface temperature. J. Geophys. Res. 86, 9776–9782.